Obtaining Spectra of Very Faint Sources with the IRS

IRS Instrument Support Team

Version 1.0: January 19, 2006

1. Introduction

In this memo, we discuss the observing and data reduction strategies recommended for ultradeep spectroscopy with the IRS. Previous IRS spectra have been limited to ~ 2 hours of on-source exposure time. To explore the limits of longer exposure times, we obtained two deep spectra in the long wavelength, low resolution module (LL). We chose different targets (at different redshifts) for each of the two sub-slits, in order to place strong emission features in their respective wavelength ranges. We also varied the observation strategy, in order to compare different approaches.

The scientific implications of the data we obtained will be presented in Teplitz et al. (2006; in preparation).

2. Target Selection and Observations

Objects were chosen from the *Hubble* Ultradeep Field area, allowing us to use the wealth of existing data from *Spitzer, Hubble,* and *Chandra* to select sources that would be both faint in the mid-infrared and have a high likelihood of detectable features in their IRS spectra. We chose integration times that would likely achieve signal to noise ratios of $\sim 2-4$ in the continuum, so that the results could be evaulated even if no emission or absorption features were detected.

For the Long-Low second order spectrum (LL-2, $14-21$ μm), we chose a target with a flux density of 0.15 mJy at 16 μm and 0.25 mJy at 24 μm. We obtained observations in *Staring Mode*. In this mode, the target is placed at two "nod" positions within the slit. The observation was broken into two AORs, each of which contained 4.5 hours of on-source integration divided between the two nod positions. At each nod position we took 70 spectra of 120 sec ramp duration. The total integration time was 9 hours. We also observed this target in the short-wavelength low-resolution slit, in the first order (SL-1), in a single AOR for three hours on source in *Staring Mode*.

For the Long-Low first order spectrum (LL-1, $21-37$ μm), we chose a second target which has a flux density of 0.05 mJy at 16 μm and 0.15 mJy at 24 μm. These observations were obtained in *Mapping Mode*, wherein the target is placed at six positions along the slit. The observations were broken into three AORs of four hours each, with 20 spectra of 120 sec ramp duration at each of the six map positions, for a total on-source integration time of 12 hours.

Observations were obtained on 06 August 2005 (SL-1), 10 August 2005 (LL-2), and 12 September 2005 (LL-1). The LL-2 AORs were executed consecutively. Two of the LL-1 AORs were consecutive, but there was a gap of more than 12 hours between the second and third observation. We observe no degradation in signal to noise resulting from the gap. All observations were scheduled immediately after the "skydark" calibrations in order to maximize the sensitivity by reducing the change of latent images from a preceding bright target. The observations are summarized in Table 1.

For long integrations, high accuracy peak-ups are strongly recommended, to guard against large deviations in telescope pointing at the cost of very little observing time. The success of the peak-up is crucial. The loss of a single AOR in a project such as this one, where the AORs are many hours in length, would be devastating. A 2MASS peak-up star was selected in SPOT for use in all AORs. We examined the MIPS 24 μm image of the star prior to submitting the AORs to ensure that it's flux was close to the SPOT prediction and that it had no bright neighbors. We selected High Accuracy PU in the blue filter. We later inspected the PU data, to check that the centroid was reasonable and that the pointing was as expected. No problems were identified.

3. Data Reduction

The Basic Calibrated Data (BCD) were produced by the S13 pipeline at the *Spitzer* Science Center (SSC), which includes ramp fitting, dark sky subtraction, droop correction,

Table 1. Observations

Obj.	z	Subslit	Mode	Ramp Time (s)	Cycles per AOR	AORs	f_{16} (mJy)	f_{24} (mJy)
1	1.09	SL-1	Staring	240	25 × 2 nods	1	0.15	0.25
		LL-2	Staring	120	70 × 2 nods	2	0.15	0.25
2	2.69	LL-1	6 × 1 map	120	20 × 6 pos.	3	0.05	0.15

linearity correction, flat fielding, and wavelength calibration. Further processing of the two dimensional dispersed frames is required before spectral extraction. In addition to the pipeline processing, we performed the following reductions:

- *Latent charge removal* A small fraction (1-2%) of charge on the detector persists between frames despite the resetting of the detector that occurs prior to every integration. This latent charge decays slowly over time and is removed by the annealing process. In the case of very faint sources, the source of latent charge is the zodiacal background. Over the course of a six hour AOR, this charge can build up to a significant level. We removed the latent signal by fitting the slope of the background detected in median of each row and subtracting that amount row-by-row from each frame. The background in BCD images is the residual after "skydark" subtraction in 3D. In the deep observations, the residual sky level was $\sim 50\ e/s$, and the latent charge built up to $\sim 5\ e/s$ by the end of the AOR (see Figure 1).

- *Rogue Pixel Interpolation* Unstable, or "rogue", pixels are those which are useable in some AORs and not in others, depending on the recent history of the detector. A mask of known rogue pixels is provided by the SSC, and we identified further suspect pixels from the data. We used the *IRSCLEAN* program provided by SSC to find rogue pixels in the 2D data. We further searched for pixels with abnormally high variance with time. Pixels identified as rogue were interpolated over using *IRSCLEAN*.

- *Residual Sky Subtraction* Once the BCD data were "cleaned", we created residual sky images from the data. In staring mode, we used the other nod position, and in mapping mode we used the other five map positions. In both cases, we used a resistant mean (removing outliers before calculating the mean) with time to calculate the sky value in each pixel.

  We experimented with using fewer of the map positions in the sky (and thus using the ones taken closest in time), but no definitive improvement was seen. Similarly, no improvement resulted from using the non-targeted subslit in the other AOR; however, the AORs were taken a month apart and were thus not optimally suited to that approach.

The individual reduced frames were coadded to produce final 2D spectra at each nod or map position. One dimensional spectra were extracted using the *SPICE* software provided by the SSC. To minimize the noise contribution from the background, we used narrower extraction windows than the default. We used a window which expanded with wavelength and had a width of ~ 2 pixels at the blue end. The "slit losses" introduced by the narrow window were estimated by extracting the spectrum of the standard star HR 7341 (taken

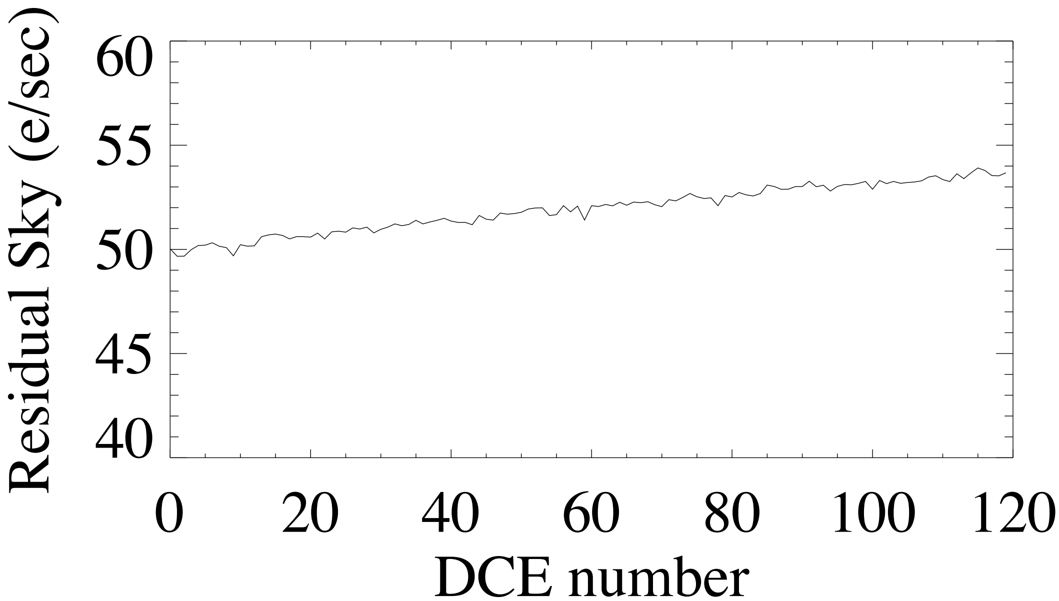

Fig. 1.— The latent charge accumulated in a pixel as a function of time (DCE number). The latent charge was measured in the median of 400 pixels.

in the same campaign) using both the standard and the new width. The correction factor varied with wavelength by $\sim 10\%$ and had a mean value of 1.4.

The signal to noise ratio (SNR) in the IRS spectra was measured using the variance with time of each pixel. We measured the variance in the sky frame for each pixel, scaled by e.g. $\sqrt{2}$ for the nodded frames, and created two dimensional noise frames for input into *SPICE*. The uncertainties were then propagated by the extraction process. These uncertainties were checked against the standard deviation in the continuum of the 1D spectra at, for example, $\sim 24\ \mu$m in LL-1.

4. Results

Figure 2 shows the 2D spectra of the sources. Several serendipitous objects are also clearly detected in the slit. Figure 3 shows the extracted spectrum of the two targets. Broad emission features, identified as polycyclic aromatic hydrocarbons (PAH) emission, are detected at rest wavelengths of 6.2, 7.7, and 8.6 μm, along with the continuum at the blue end of LL-2 and LL-1. The continuum level is in good agreement with the estimate from

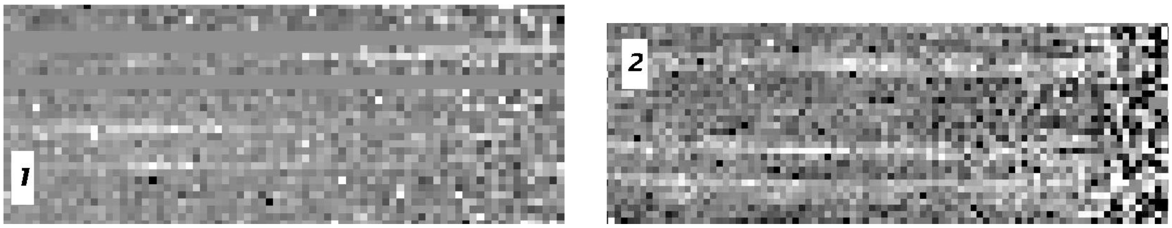

Fig. 2.— The 2D dispersed frame image of the IRS spectra of faint sources. The left panel shows the LL-2 spectrum of Source 1. The source is the bottom of the three detected objects. The right panel shows the LL-1 spectrum of Source 2. The source is the top of the three detected objects, as labelled. In each case, only the illuminated portion of the relevant order is shown. Wavelength runs from blue on the left to red on the right.

the broad-band photometry at 16 and 24 μm. The SL spectrum of Source 1, which is quite red, is considerably noisier given the shorter integration time, but it was not the main focus of the test discussed here, and is not shown in the figure.

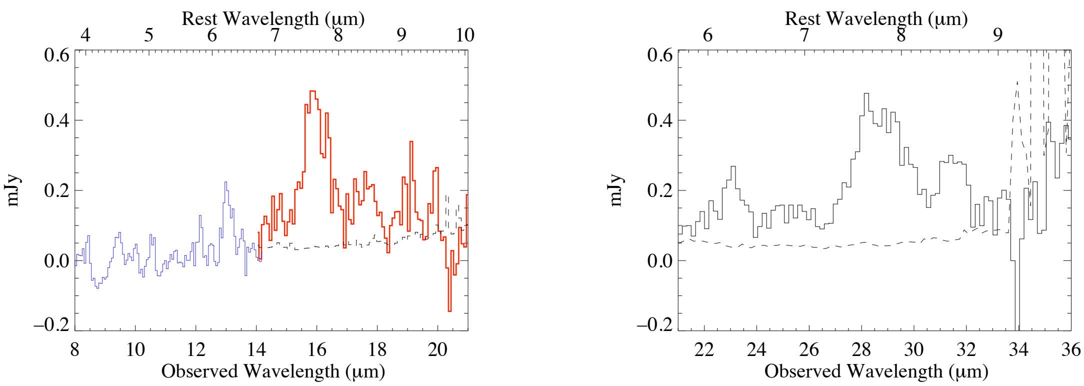

Fig. 3.— The IRS spectra of faint sources. The left panel shows the SL-1 (thin line) and LL-2 (thick line) spectra of Source 1. The right panel shows the LL-1 spectrum of Source 2. The 1σ LL error arrays are shown (dashed lines).

The SNR at 16 μm in LL-2 and 24 μm in LL-1 is generally consistent with the predictions of *SPEC-PET* on the SSC website (see Table 2). We remind all observers that the *SPEC-PET* predictions do not include noise introduced by the pipeline processing or spectral extraction. They also assume the spectra are smoothed to R=50, which we have not done. *SPEC-PET* predicts a 12 hour integration in LL-1 will yield a 3σ uncertainty of 0.12 mJy at 24 μm with spectral resolution smoothed to R=50. Our measured 3σ uncertainty is $\sim$ 0.13 mJy. *SPEC-PET* predicts a 9 hour integration in LL-2 will yield a 3σ uncertainty of 0.08 mJy at 16 μm and R=50. Our measured uncertainty is $\sim$ 0.12 mJy. While both spectra have noise values close to the *SPEC-PET* prediction, the *Mapping Mode* observation gives noticeably better results. **We therefore recommend spectral mapping along the slit for observations of faint sources.**

The SNR varies strongly with wavelength. The noise rises sharply at the red end of each order. The shape of the error array measured in our data agrees well with the predictions of *SPEC-PET*, independent of the overall level.

Figure 4 shows the improvement with time obtained by extracting the spectrum from fractions of the LL-1 data. The data were re-reduced using only the number of DCEs for each case. The SNR scales with time as expected.

5. Requesting Long Spectra

Long spectra may be planned using the standard AOTs available in SPOT. There is a six hour limit per AOR, so long spectra should be divided into multiple AORs if necessary. We chose, for example, to divide a twelve hour (on source) spectrum into three equal length AORs instead of six hour AORs and a slightly shorter one. Care should be taken to use consistent PU parameters in each AOR.

One special request should be made when planning long spectra. The danger of latent charge from bright objects in preceeding observations can be mitigated by scheduling long spectra immediately after the "skydark" calibrations. This request should be noted and justified in the Technical Justification of the proposal. In addition, this scheduling request should be noted in the *Comments* field in the SPOT *AOR* screen. The scheduling request should be the first comment, and should say (exactly) **"PUT IMMED. AFTER DARKCAL"**.

Table 2. Comparison with SPEC-PET

AOT	Order	wavelength	itime hours	SPEC-PET (R=50) 3σ Uncertainty	Measured (R$\sim$ 80) 3σ Uncertainty
Staring Mode	LL-2	16 μm	9	0.08 mJy	0.12 mJy
Mapping Mode	LL-1	24 μm	12	0.12 mJy	0.13 mJy

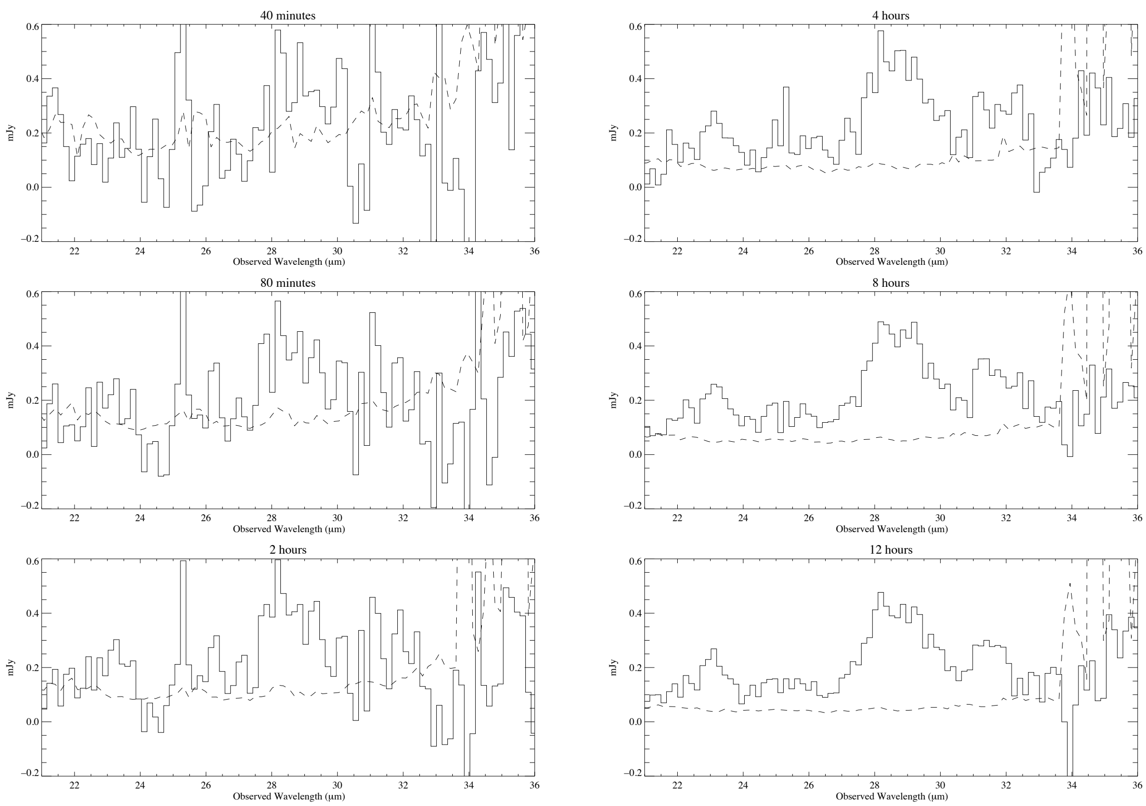

Fig. 4.— The extracted spectrum of Source 2 as a function of integration time. In each panel the spectrum is shown extracted from a subset of the data, along with the corresponding 1σ uncertainty (dashed line).